

THERMAL ANALYSIS OF HEATING–COOLING MAT OF TEXTILE INCUBATOR FOR INFANTS

Zbigniew Mikołajczyk^{1,*}, Agnieszka Szalek²

¹ Department of Knitting Technology and Textile Machines Lodz University of Technology, Lodz, Poland

² Łukasiewicz Research Network - Institute of Biopolymers and Chemical Fibres Lodz, Poland

*Corresponding author. E-mail: zbigniew.mikolajczyk@p.lodz.pl

Abstract:

On the medical device market there are several types of stationary and portable incubators that can be used in the care of infants. The prototype of a textile incubator made as part of this work consists of five material layers. The textile incubator is equipped with a functional heating and cooling mat, which is made on the basis of 3D channeled weft-knitted fabric. Its function is to generate heat and maintain it inside the textile incubator or to cool the baby's body while using therapeutic hypothermia. The mat is equipped with hoses transporting the heating or cooling medium.

The mat, depending on variable input parameters, can emit heat in the range from 1.15 W to 86.88 W. In case of the cooling function, it can receive heat in the range from –4.32 to –27.96 W. This indicates a large adjustment range of the amount of heat supplied and received, which is a positive feature, and enables programming the heat balance to ensure comfort for the baby.

The analysis of temperature measurements on the mat surface confirmed that maximum temperature differences do not exceed 1.6°C.

Keywords:

Heating-cooling mat, textile incubator, thermal analysis, thermal comfort, knitted fabric

1. Introduction

Poland, just like other developing countries in the world, has been struggling for several years with the problem of low birth rate. Data published by European and world health organizations show that since 1990 the number of births has been steadily decreasing, which poses the risk of lack of generational replacement [1]. According to Polish Central Statistical Office, at the end of 2017, the total population of Poland was 38,434,000, and the number of births was 0.5 thousand lower than the number of deaths [2, 3].

At present, medicine is able to keep alive and provide appropriate care for babies born prematurely in the 21st week of pregnancy [4]. Such an infant is not able to survive alone outside the mother's body, as it is completely undeveloped and not adapted to life outside. Premature babies born after the 25th week of pregnancy have the greatest chance of survival [5]. However, most of them have underdeveloped organs, and require special care and medical supervision, so for the first days or even months of their lives they remain in incubators, in which constant temperature and high humidity are maintained. The incubator also ensures the right amount of oxygen, because premature babies have less ability to absorb it. In the incubator the air is saturated with steam, which protects the delicate skin of the baby from drying out [6].

Premature infants cannot maintain proper body temperature on their own. They have insufficiently developed subcutaneous fat, and their muscles are too weak to produce heat. Problems with body temperature regulation and disturbances in the water and electrolyte balance appear due to the fact that the amount of adipose tissue is small [7, 8]. Maintaining proper thermoregulation is the key element in caring for premature babies. The optimal temperature for a newborn is such ambient temperature in which deep body temperature at rest ranges from 36.7°C to 37.3°C [9, 10].

A related topic concerning thermoregulation in the environment in which the infant is located is the issue of therapeutic hypothermia. In case of this phenomenon, the situation is completely reversed. One of the basic aims of the incubator is warming up the infant's body when it suffers energy losses not balanced by the heat generated during metabolic process [11].

The main purpose of therapeutic hypothermia in full-term newborn babies is to prevent secondary damage to nerve tissue caused by perinatal hypoxia. In recent years, apart from pharmacological neuroprotection, a relatively new method has been implemented, based on usage of the neuroprotective effect of controlled reduction of deep body temperature-hypothermia [12]. Hypothermia consists in cooling the inside of the body to a temperature <35°C. The neuroprotective



mechanism of hypothermia consists in slowing down the metabolism, and thus reducing the energy needs of nerve cells (temperature drop by 1°C reduces metabolism by 5%, which decreases the loss of energy reserves of the cells). Additionally, hypothermia inhibits the cascade of biochemical reactions occurring after hypoxic-ischemic injury [13]. In case of moderate hypothermia therapy, two types of methods are used, which differ in reaching the therapeutic temperature. The first method involves selective brain cooling. At the same time, research works are carried out on the second method, based on using general hypothermia in the therapy of hypoxic newborns. This therapy involves cooling the whole body, until the inside temperature drops to $33^{\circ}\text{C} \pm 0.5^{\circ}\text{K}$. This temperature range is applied in moderate and mild hypothermia [14]. The problem of neonatal hypothermia has been considered taking into account the new approach to the functions of a textile incubator model, which is the theme of this publication [15].

The first incubator for premature newborns was created by the French obstetrician Stephane Tarnier, who worked in the maternity ward of a Paris hospital [16].

Tarnier and Martin's incubator built in 1883 consisted of two chambers: in the bottom one, water was heated with the help of an oil lamp, and then it was giving heat to the child lying in the upper chamber. Modern incubators are complex medical devices which ensure comfort and proper environment for the baby and fulfill many other therapeutic and diagnostic functions. Open, closed, and hybrid incubators are currently used to take care for newborns [17].

1.1. Basic assumptions for the construction and functional characteristics of a textile incubator

As a result of the analysis of neonatal physiology and therapeutic methods of taking care for newborns, including the use of classic incubators and other medical devices, an innovative concept for building a functional model of a textile incubator has been developed. This incubator is not going to replace the well-known stationary, open, or closed incubators. It will fulfill other functions in therapeutic care for newborns. The main function of the textile incubator will be to create optimal conditions for physiological comfort in terms of body thermal balance. The incubator will also be useful in the process of cooling the newborn's body during hypothermia therapy. The assumptions regarding the construction and functional characteristics of the textile incubator were developed in cooperation with the medical environment of the Neonatology Clinic of the Polish Mother's Memorial Hospital Research Institute in Łódź. We would like to give special thanks to the head of the clinic, Prof. Ewa Gulczyńska, MD, Ph.D. and Ms. Wioletta Cedrowska – Adamus, MA, a member of the Board of the Polish Society of Neonatological Nurses and Midwives. According to the doctors, the textile incubator is a desirable and practical solution in taking medical care for newborns in the following therapeutic cases:

1. during the examination and assessment of the condition of newborn infants immediately after delivery,
2. during thermal stabilization consisting in heating the body using a heating mat,
3. while transporting a newborn baby in an ambulance and between hospital departments,
4. during therapeutic hypothermia,
5. while acclimatizing the baby to ambient conditions after it has been removed from the closed incubator,
6. during laser therapy used to reduce high bilirubin level in the blood,
7. during oxygen and other aerosol therapy with simultaneously heating the newborn, and
8. during surgery in newborns affected by various diseases.

The textile incubator consists of five layers, where the outer layer fulfills insulating function, the next layer is made of metalized polyester film to prevent heat loss through radiation outside the textile incubator, and the third layer is the active functional heating and cooling mat. Layer 4 is a vapor-permeable membrane attached to Layer 5 – a soft fabric made of organic cotton, natural silk, or textured polypropylene. Layers 4 and 5 are disposable elements to ensure proper hygiene standards. After designing the structure of the textile incubator, a prototype was prepared, which is shown in Figure 1.



Figure 1. Prototype of textile incubator. *Source:* authors' own studies.

2. Construction of the heating and cooling element of the textile incubator

At the initial stage of defining the assumptions for the construction of the heating and cooling element, two system solutions were adopted to control the amount of supplied and received heat. In the first variant, it was decided to divide the incubator into three heating zones: for the head, the torso, and the legs. This division resulted from different phenomena and amount of heat exchange for individual body segments of the newborn. It was assumed to construct separate heating and cooling elements for the three zones of the incubator. The second proposal was to average the heating zone and build one heating and cooling element, covering the entire inner surface of the device. The first concept was rejected by the medical community, which pragmatically supported the second variant of the incubator construction. The construction of the heating and cooling element was a separate technical problem. Four concepts were analyzed, including a classic electric heater using Joule–Lenz law to convert electricity into thermal energy; heat pump in the form of a Peltier element; a radiator with a heat carrier in the form of hot water, giving up thermal energy as a function of the difference in specific enthalpy of water for the temperature of the heater and the temperature of the environment; and a heater emitting infrared radiation in the adjustable wavelength range. Due to the fact that the thermal mat should fulfill both heating and cooling functions, only two of the presented proposals were taken into account. These were the Peltier heat pump and the radiator with water jacket. Finally, the solution accepted by the medical community was the heating and cooling mat with distilled water as the exchanger transporting the heat flux. In addition, in the design of the textile incubator, it was decided to use an infrared heat radiator with wavelength of 780–2,500 nm as a complementary heating element, and optical fiber emitting ultraviolet radiation in a wavelength range of 450–470 nm used in the treatment of hyperbilirubinemia.

2.1. Construction of the channeled mat

The channeled mat with adjustable heat exchange system was made on the basis of a three-layer 3D weft-knitted fabric, with longitudinal channels in the inner layer. Hoses with heating and cooling liquid were placed inside the channels (Figure 2).

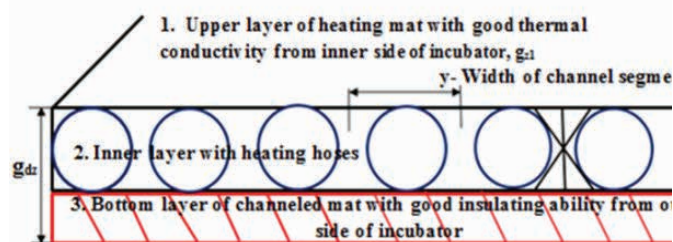


Figure 2. Construction of heating-cooling mat.

The following symbols were adopted in the geometric model of the knitted channeled mat:

$g_{z1} \gg 0$ - thickness of the outer layer of the mat with low cover factor and thermal resistance, so that as much heat as possible is transferred from the heating medium towards the baby;

g_{z2} - thickness of the outer layer (bottom of the channeled mat) with best thermal insulation ability;

g_{dz} - thickness of knitted channeled mat;

$g_w = d_{sr}$ - thickness of the inner layer of the mat, equal to the outer diameter of the hose distributing the heating-cooling medium;

y - width of channel segment.

Several variants of the channeled knitted mat were designed and produced on a flat weft-knitting machine and a circular double-knitting machine. Five variants of the channeled fabrics were made on a flat weft-knitting machine Stoll type CMS 530 with needle gauge E5 and fabric density was set on the

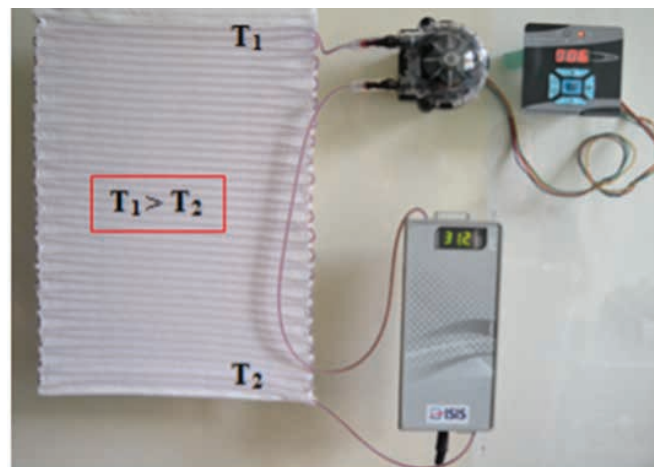
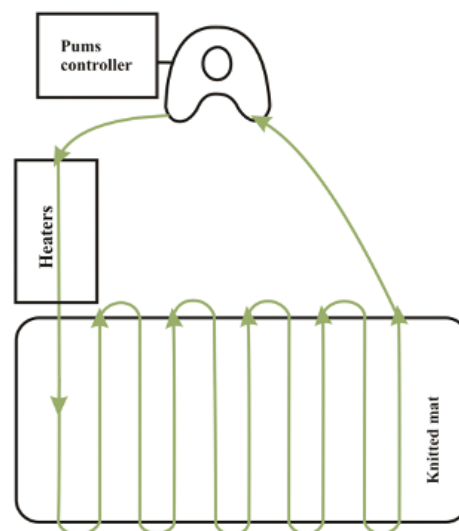
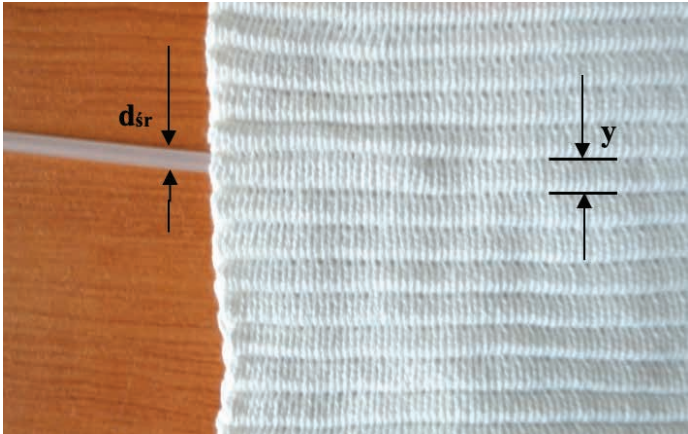


Figure 3. Mat construction with one hose interlaced in each channel (a) heating diagram (b) test stand for measuring temperature distribution. Source: authors' own studies.

Table 1. Channeled weft-knitted fabric made on Stoll flat weft-knitting machine Stoll.

No.		Stroke direction		Stitch
a)	1	←	x1	
	2	→	x1	
	3	←	x1	
	4	→	x1	
	5	← →	x7	
	6	→	x1	
	7	← →	x7	
	8	→ ←	x4	
b)				<p>Fabric parameters:</p> <p>Fabric thickness: 5 mm</p> <p>Mass per unit area: 871 g/m²</p> <p>Weft density: 80 course./ 10 cm</p> <p>Wale density: 30 wale/ 10 cm</p> <p>Raw material- cotton</p> <p>Channels diameter: $d_{sr} = 4$ mm</p> <p>Channel segment width: $y = 5$ mm</p>

machine 3.5. The raw material used for the samples was cotton yarn with linear density of 32 x 2 tex. The channeled knitted fabrics were made with the use of additional courses on a single needle bed. The knitted fabrics differed in the diameter of the channels and the width of the segments. Some examples of the stitch variants are shown in Table 1.

In the next stage three variants of a channeled mat were made on a circular double-knitting machine MAYER & Cia. with the following technical parameters: knock-over depth for cylinder needles, 25; knock-over depth for disc needles, 20; straight line distance between the disc and the cylinder, 3.5 mm; knitting speed, 11 rot/min; monofilament feeding rate, 192 m/min; monofilament take-up, 8 mm per one needle; raw materials used: polypropylene 84 dtex f 25, polyester 75 den x 2, polyester 100 den x 1, and polypropylene monofilament with a diameter of 0.08 mm. Three variants of the knitted channeled

mat with the same stitches were produced, differing only in the width of the channel segments.

Table 2 presents schematic stitch record of the channeled knitted mat and Figure 3 shows its actual view.

The next step was designing the arrangement of hoses transporting the heating medium inside the mat channels. A 50 x 30 cm sample was made on a circular double-knitting machine. First, the heating mat through which one hose was interlaced, and thus one heating zone was obtained, was subjected to preliminary tests of temperature distribution (Figure 3).

As a result of the tests, it turned out that the inlet temperature $T_1 = 25.3^\circ\text{C}$ is higher than the exit temperature $T_2 = 23.5^\circ\text{C}$. The temperature difference was 1.8°C , at external temperature

Table 2. Stitches of the channeled mat. The figure of the stitch in the table.

No.		Rotation number	Stitch	Disc/ cylinder	Stitch type	Comments
a)	1	x2 or x 4		T	Plain stitch on disc needles	Connections between outer layers of the fabric
			C	Plain stitch on cylinder needles		
			T	Tuck loops connecting the layers		
			C	Plain stitch on disc needles		
			T	Plain stitch on cylinder needles		
			C	Tuck loops connecting the layers		
			T			
			C			
	2	x7 up to 13		T	Plain stitch on disc needles	Outer layers of the channels
			C	Plain stitch on cylinder needles		
			T			
			C			

b)		<p>Averaged parameters of the channeled fabric:</p> <table><tr><th><u>Parameters of a sample 50 x 30 cm:</u></th><th><u>Averaged values</u></th></tr><tr><td>mat weight without hose,</td><td>26.31 g</td></tr><tr><td>mat weight with hose</td><td>254.49 g</td></tr><tr><td>mat thickness without hose</td><td>2.35 mm</td></tr><tr><td>mat thickness with hose</td><td>6.29 mm</td></tr><tr><td>weft density Pr of the fabric</td><td>155 course/10 cm</td></tr><tr><td>wale density Pk of the fabric</td><td>109 wale/10 cm</td></tr><tr><td>fabric mass per unit area, Mp</td><td>184.37 g/m²</td></tr><tr><td>loop width A</td><td>0.92 mm</td></tr><tr><td>loop height, B</td><td>0.67 mm</td></tr><tr><td>loop shape ratio, C</td><td>0.72</td></tr><tr><td>channels diameter, d_{gr}</td><td>5 mm</td></tr><tr><td>Distance between channels,</td><td>y 7 mm</td></tr></table>	<u>Parameters of a sample 50 x 30 cm:</u>	<u>Averaged values</u>	mat weight without hose,	26.31 g	mat weight with hose	254.49 g	mat thickness without hose	2.35 mm	mat thickness with hose	6.29 mm	weft density Pr of the fabric	155 course/10 cm	wale density Pk of the fabric	109 wale/10 cm	fabric mass per unit area, Mp	184.37 g/m ²	loop width A	0.92 mm	loop height, B	0.67 mm	loop shape ratio, C	0.72	channels diameter, d _{gr}	5 mm	Distance between channels,	y 7 mm
	<u>Parameters of a sample 50 x 30 cm:</u>		<u>Averaged values</u>																									
mat weight without hose,	26.31 g																											
mat weight with hose	254.49 g																											
mat thickness without hose	2.35 mm																											
mat thickness with hose	6.29 mm																											
weft density Pr of the fabric	155 course/10 cm																											
wale density Pk of the fabric	109 wale/10 cm																											
fabric mass per unit area, Mp	184.37 g/m ²																											
loop width A	0.92 mm																											
loop height, B	0.67 mm																											
loop shape ratio, C	0.72																											
channels diameter, d _{gr}	5 mm																											
Distance between channels,	y 7 mm																											
c)																												

Figure 3. Channeled knitted mat a) view from above
b) intersection of knitted heating mat
Source: authors' own studies.

$t_z = 21^\circ\text{C}$. The aim of the project was to maintain constant heat distribution over the entire surface of the mat. In further research, the mat was divided into two heating zones, and two hoses were interlaced alternately at every other channel (Figure 4). A plastic hose with a diameter of 5 mm made of PVC with thermal conductivity of $0.17 \text{ W/m}^\circ\text{K}^{-1}$ was introduced into the channels and heated distilled water was flowing through.

The second model is a mat with a flexible silicone hose with thermal conductivity of $0.24 \text{ W/m}^\circ\text{K}^{-1}$. In this case, the heating medium was delivered with a separate collector supplying individual heating tubes.

The reception of the heating medium was realized by a parallel receiving collector (Figure 5). Two variants of the mat were designed and constructed. In both variants, 16 temperature sensors monitoring temperature distribution were arranged on

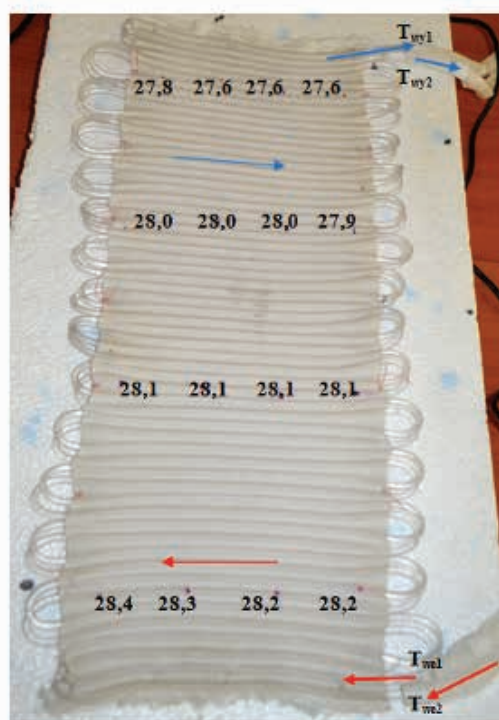
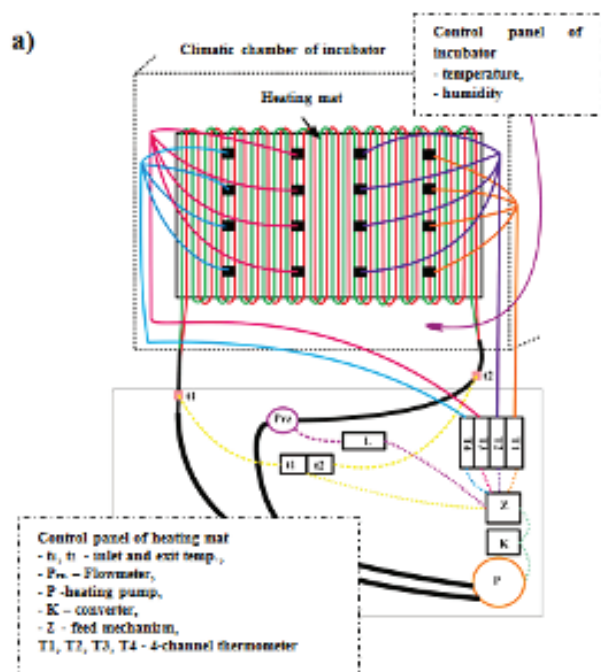


Figure 4. Mat construction with two hoses interlaced every other channel: (a) heating diagram, (b) mat photo. Source: authors' own studies.

the surface of the heating-cooling mat. For further research, both variants of the channel mat were used, with different ways of interlacing the hoses in the channels.

2.2. Construction of a test stand for thermal analysis of the heating mat

The test stand shown in Figure 6 consists of the following elements, marked with numbers from 1 to 5:

1. Two incubators:

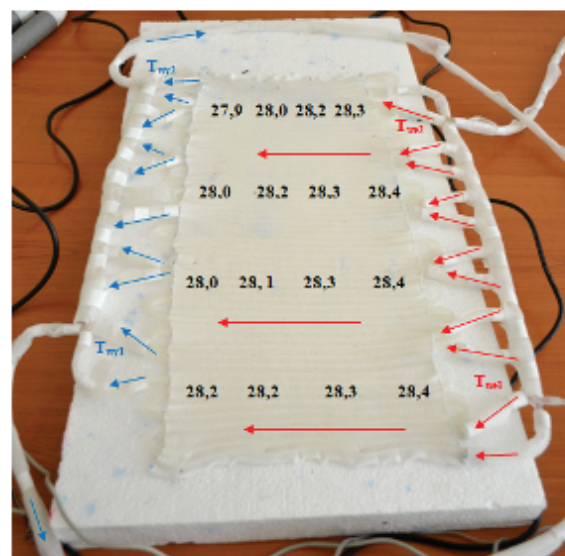
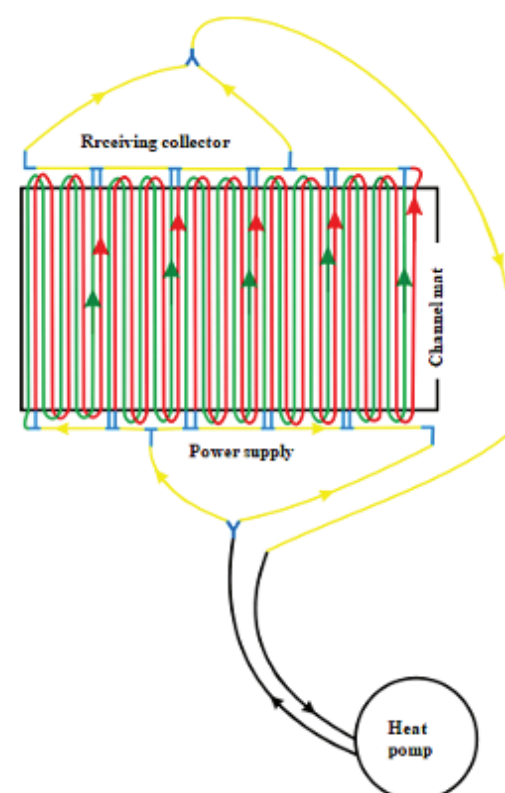


Figure 5. Channeled mat with two collectors: (a) heating mat diagram, (b) mat photo. Source: authors' own studies.

- V – 850 incubator, made by Atom Medical Corporation, in which temperature can be controlled in the range from 25°C up to 37°C. It was used for the tests at low outside temperature – 25–28°C and humidity 70%. It can be used to maintain stable environment with predefined temperature and humidity, and the microclimate inside the incubator is controlled using the control panel.
- Isolette C 2000 incubator made by Dräger, in which air temperature can be adjusted in the range from 28.0°C to 37.0°C, and humidity in the range from 30% to 95%. This incubator was used for testing at higher outside temperatures: 28–37°C.

2. Channeled knitted mat with heating medium equipped with 16 temperature sensors, which was placed inside the incubator chamber. Two variants of channeled mats were used in the tests. In the first mat the hose was interlaced every other channel, and the second variant was.
3. The HTP-1500 heat pump from Android Medical System, which functioned as a heating device that was used to supply the heated or cooled water to the inside of the channeled mat. This device is frequently used in heat therapies. The pump heats distilled water to 24–41°C and has two degrees of protection against overheating, at 43°C and 46°C, with temperature setting accuracy of $\pm 2^\circ\text{C}$. To avoid temperature differences and cooling down of the liquid, the hoses transporting the heating medium were insulated with a polyethylene foam cover.
4. A flow meter, which records the instantaneous flow of the liquid inside the tube in liters or cubic meters per time unit, namely seconds, minutes, and hours.
5. A four-channel 12 V measuring unit, recording the temperature on the surface of the mat placed inside the incubator. The temperature range that can be measured is from -50°C to $+125^\circ\text{C}$. DS18B20 thermal sensors with measurement accuracy up to 0.1°C were used. The constructed measuring stand was used to analyze the amount of heat emitted by the heating-cooling mat and temperature distribution on the mat surface.

3. Thermal analysis of the heating-cooling mat

The analysis of the heating power of the mat and temperature distribution on its surface was carried out in two separate stages. In the first stage, two methods were used to calculate the amount of heat emitted by the “radiator”. In the second stage, the analysis of temperature surface distribution was performed using a traditional method of temperature measurement with contact sensors and non-contact thermal imaging.

3.1. Analysis of heating power of the heating-cooling mat

The first method of calculating the heating power is based on the operating principle of heating installations, where heat can be transferred only in the direction of temperature drop. In this case, the heat carrier is hot water (distilled water), which is continuously transported between the heat source, where it heats up to t_1 , and the heat receiver, where it is cooled down to temperature t_2 , emitting a certain amount of heat Q to the environment. The amount of heat Q supplied to the receiver in the time from τ_0 to τ_1 can be calculated from the formula [18]:

$$Q = \int_{\tau_0}^{\tau_1} q_m (h_1 - h_2) d\tau \quad (1)$$

where q_m represents the mass flow of heat carrier; h_1 the specific enthalpy of heat carrier at higher temperature t_1 and the corresponding pressure; and h_2 the specific enthalpy of heat carrier at lower temperature t_2 and the corresponding pressure.

However, to simplify the measurements and the related calculations, the heat ratio k was introduced, which is

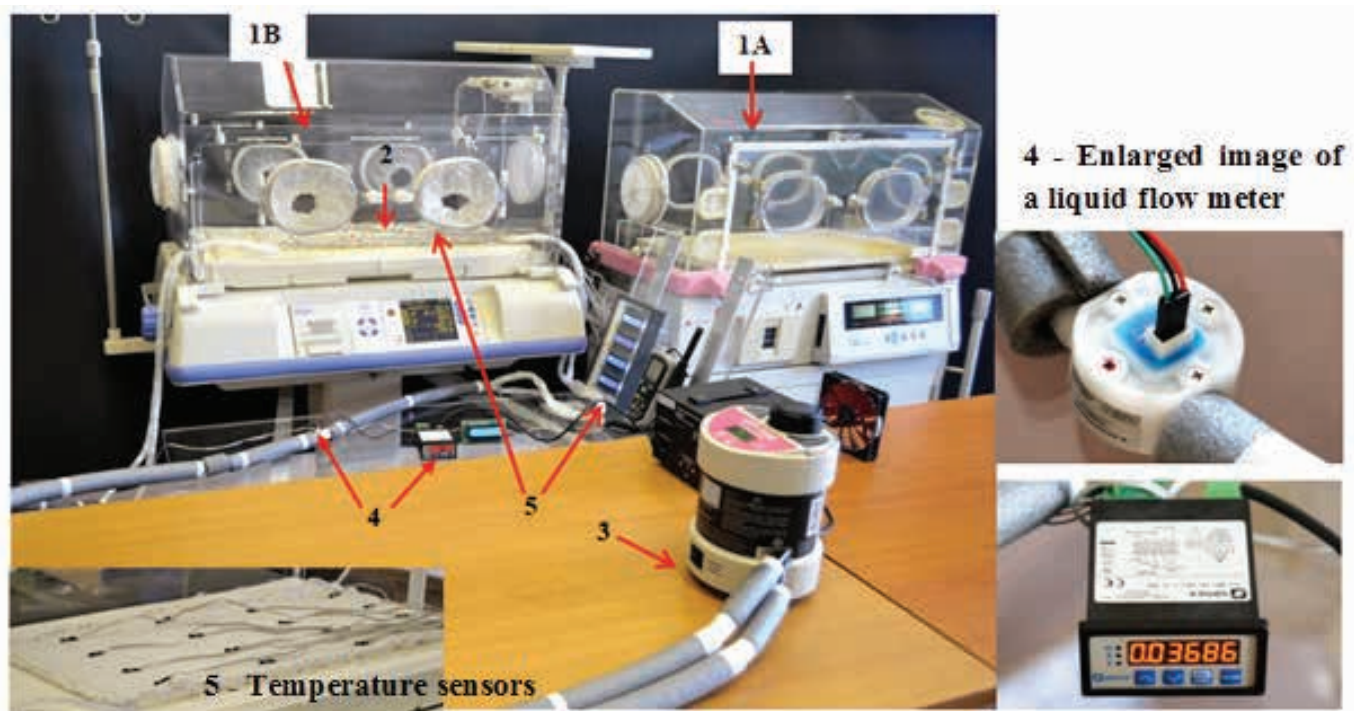


Figure 6. Construction of measuring stand for thermal analysis of heating mat. *Source:* authors' own studies.

equivalent to the physical quantities of the heat carrier and its temperatures, and is expressed as:

$$k = \rho \left(\frac{h_1 - h_2}{t_1 - t_2} \right) \quad (2)$$

where ρ is the density of the heat carrier and is equal to the amount of heat exchanged with the environment by 1 m³ of energy carrier, under appropriate conditions when the temperature changes by 1 K [19]. The amount of heat Q is simply dependent on volume V of the energy carrier which flowed through the receiver during the measurement, according to the formula:

$$Q = \int_{V_2}^{V_1} k(t_1 - t_2) dv \quad (3)$$

Formula (3) can be simplified, assuming a steady state in the heating installations. With this assumption, the correct amount of heat Q_c supplied to the receiver by the energy carrier with volume V can be calculated from the formula:

$$Q_c = kV(t_1 - t_2) \quad (4)$$

Formula (4) can also be used in case of heat transfer, i.e., to calculate the amount of heat absorbed by the carrier [20].

Formula (4) was used to analyze the amount of emitted heat – i.e., the mat-heating power.

Table 3 below presents the results of calculations of heat emitted by the heating mat with a hose interlaced every other channel, made according to the first method. Calculations of heat emitted by the heating and cooling mat were made on the basis of the inlet and exit temperatures of the medium – T_{we} and T_{wy} and the velocity of water flow of volume V' through the heating-cooling mat was located in a climate chamber, which was a closed incubator. The temperature in the incubator ranged from 24°C to 35°C, and a constant humidity of 70% was maintained, which corresponds to the actual climate conditions inside the incubator for neonatal care.

As a result of the tests, it can be noticed that heat expenditure of the mat for empirically set temperature differences Δt and flow rate V of the heating medium is in the range from 2.66 W to 31.85 W. It should be emphasized that determining the difference Δt in the range from 0.1°C to 1.1°C resulted from the adopted air parameters inside the incubator and the settings adjusted automatically to obtain repeatability of temperatures of the heating medium in the heating-pumping device. High values of heat expenditure in the range of 13.90–31.85 W are marked in yellow. The last column of the table presents average temperatures on the mat surface, which vary from 28.1°C to 37.4°C. The average temperatures on the mat surface, close to the physiological temperature of premature babies, which equals 35.5°C, are marked in green. The temperature on the mat surface was measured using 16 sensors arranged on the mat.

The heat transfer from the mat to the inside of the textile incubator can also be calculated using the second method mentioned above. When the temperature of the fluid flowing through the hose is different from the temperature of its walls, then heat transfer can be observed between the hose walls and the fluid. This transfer occurs on the solid–fluid interface. The intensity of this transfer is proportional to the product of the interface equal to the wall surface of the hose and the characteristic difference of the wall and fluid temperatures. This relationship is expressed by the Newtonian equation [21]:

$$Q_{c2} = \alpha \cdot A \cdot \Delta T \quad (5)$$

where Q_{c2} represents heat flux whose direction is in accordance with the direction of temperature gradient; W , A heat exchange area, m²; ΔT temperature difference of exchanger wall and fluid (or vice versa); and K , α heat penetration coefficient, W/m²K.

The amount of heat transmission calculated according to the second method, for the selected mat samples where the hose interlaces every other channel, is close to the amount of heating power calculated by the first method. The differences in the calculations of the heating power Q_{c1} and Q_{c2} did not exceed 6.7%. An analysis was carried out of simulation calculations of the amount of emitted heat for different flow rates of the heating medium. The calculations presented in Table 3 were made for $V' = 0.024$ m³/h. In the functional analysis $Q_{c1} = f(V')$, the values V' were assumed at the level of 0.01 m³/h and 0.075 m³/h. The results of the calculations are presented in Tables 4 and 5.

From the obtained data, it can be inferred that the heating power of the mat is significantly affected by the flow rate of the medium. When its speed increases, the heating power of the mat increases; vice versa, decreased flow rate of the medium results in decreased heating power. These relationships are also a function of the temperature inside the incubator. This inference is very important regarding the possibility of regulating the amount of heat generated by the heating and cooling mat in a textile incubator. Using an appropriately selected automation system, it is possible to regulate the amount of heat emitted (received) by the mat and thus control the body temperature and thermal comfort of the child. An analysis was also made of the amount of heat emitted by the mat with a different structure than the one previously considered. This mat has two longitudinal collectors supplying and collecting the medium, and silicone heating hoses perpendicular to the collectors. Calculations of the amount of emitted heat were carried out using the first method (Relationship 4). The calculated amounts of heat expenditure are given in Table 6.

As a result of the research, it was found that heat expenditure is within the range from 2.67 W to 20.26 W. High values of heat expenditure in the range of 11.13–20.26 W are marked in yellow and the lowest values 2.67–2.89 W in pink. The last column shows average temperatures on the mat surface, which range from 27.9°C to 36.5°C. Average temperatures on the surface of the mat, which are close to the infant's physiological temperature of 35.5°C, are marked in green. During the study, it was observed that in case of the second variant of mat construction there was a slight increase in the flow rate of the

Table 3. Amount of heat emitted by mat where hose interlaces every other channel.

Temp. inside incubator, °C	Air humidity, %	Pump temp, °C	Inlet temp., °C	Exit temp., °C	Temp. difference. Δt , K	Water flow rate V' , m ³ /h	Heat ratio for water MJ/m ³ K	Amount of heat emitted by mat Q_{c1} , W	Average mat temp., °C
23.7	27.4	30	29.3	28.8	0.5	0.024	4.1711	13.90	28.1
23.9	26.5	35	33.1	32.3	0.8	0.024	4.1711	22.24	31.0
24.0	27.0	41	37.8	36.8	1.0	0.025	4.1704	28.96	35.2
25.6	70.0	30	29.0	28.7	0.3	0.023	4.1711	7.99	28.2
25.9	70.0	35	33.0	32.2	0.8	0.024	4.1711	22.24	31.1
25.8	70.0	41	37.5	36.6	0.9	0.025	4.1704	26.06	34.8
26.0	70.0	30	29.1	29.0	0.1	0.023	4.1711	2.66	28.9
26.1	70.0	35	33.8	32.7	1.1	0.024	4.1711	31.85	31.5
26.3	70.0	41	37.1	36.5	0.6	0.025	4.1704	17.38	34.9
27.0	70.0	30	29.6	29.3	0.3	0.023	4.1711	7.99	28.1
27.1	70.0	35	33.0	32.3	0.7	0.024	4.1711	19.46	31.5
27.9	70.0	41	37.1	36.9	1.0	0.025	4.1704	28.96	35.3
28.0	70.0	30	29.5	29.3	0.2	0.023	4.1711	5.33	29.7
28.4	70.0	35	32.8	32.3	0.5	0.024	4.1711	13.90	32.5
28.9	71.0	41	37.6	36.8	0.8	0.025	4.1704	23.17	35.8
29.0	70.0	30	29.8	29.6	0.2	0.023	4.1711	5.33	28.3
29.0	70	35	32.8	32.3	0.5	0.024	4.1711	13.90	32.1
29.2	70	41	37.6	36.8	0.8	0.025	4.1704	23.17	35.7
30.1	70	35	32.8	31.3	0.5	0.024	4.1711	13.90	31.9
30.4	72	41	37.9	37.2	0.7	0.025	4.1595	20.22	35.8
31.1	71	35	33.4	32.8	0.6	0.024	4.1711	16.68	33.4
31.2	70	41	38.0	37.1	0.9	0.025	4.1595	26.00	36.9
32.1	70	35	33.3	32.9	0.4	0.023	4.1711	10.66	31.7
32.2	70	41	38.0	37.3	0.7	0.024	4.1595	19.41	35.2
33.0	70	35	33.4	32.6	0.8	0.024	4.1711	22.24	30.6
33.2	70	41	37.8	36.8	1.0	0.025	4.1595	28.88	37.4
35.0	70	41	37.8	37.1	0.7	0.025	4.1595	20.21	36.3

Table 4. Simulation of changes in mat heating power with reduced flow rate $V' = 0.01$ m³/h.

Temp. inside incubator, °C	Air humidity, %	Pump temp., °C	Inlet temp., °C	Exit temp., °C	Temp. difference, Δt , K	Water flow rate V , m ³ /h	Heat ratio k , for water MJ/m ³ K	Amount of heat emitted by mat Q_{c1} , W
26.3	70	41	37.1	36.5	0.6	0.01	4.1704	6.93
27.1	70	35	33.0	32.3	0.7	0.01	4.1711	8.08
28.4	70	35	32.8	32.3	0.5	0.01	4.1711	5.77
29.2	70	41	37.6	36.8	0.8	0.01	4.1704	9.24
31.2	70	41	38.0	37.1	0.9	0.01	4.1595	10.36
32.1	70	35	33.3	32.9	0.4	0.01	4.1711	4.62
33.2	70	41	37.8	36.8	1.0	0.01	4.1595	11.52

Table 5. Simulation of changes in mat heating power with increased flow rate $V' = 0.075 \text{ m}^3/\text{h}$.

Temp. inside incubator, °C	Air humidity, %	Pump temp., °C	Inlet temp., °C	Exit temp., °C	Temp. difference, Δt , K	Water flow rate V , m^3/h	Heat ratio k , for water $\text{MJ}/\text{m}^3\text{K}$	Amount of heat emitted by mat Q_{c1} , W
26.3	70	41	37.1	36.5	0.6	0.075	4.1704	52.12
27.1	70	35	33.0	32.3	0.7	0.075	4.1711	60.82
28.4	70	35	32.8	32.3	0.5	0.075	4.1711	43.44
29.2	70	41	37.6	36.8	0.8	0.075	4.1704	64.49
31.2	70	41	38.0	37.1	0.9	0.075	4.1595	77.97
32.1	70	35	33.3	32.9	0.4	0.075	4.1711	34.75
33.2	70	41	37.8	36.8	1.0	0.075	4.1595	86.64

Table 6. Amounts of heat emitted by mat with two collectors.

Ambient temp., °C	Air humidity, %	Temp. of heating medium, °C	Inlet temp., °C	Exit temp., °C	Temp. difference, Δt , K	Water flow rate V' , m^3	Heat ratio k , $\text{MJ}/\text{m}^3\text{K}$	Amount of heat emitted by mat Q_{c1} , W	Average mat temp., °C
23.2	43.6	30	29.0	28.8	0.2	0.023	4.1711	5.33	27.9
23.2	43.2	35	32.6	32.2	0.4	0.024	4.1711	11.13	30.8
23.5	43.1	41	37.4	36.7	0.7	0.025	4.1704	20.26	34.6
25.4	70.0	30	29.1	29.0	0.1	0.024	4.1711	2.78	28.4
25.7	70.0	35	33.0	32.6	0.4	0.025	4.1711	11.58	31.3
25.9	70.0	41	37.8	37.2	0.6	0.026	4.1704	18.07	35.3
26.2	70.0	30	29.6	29.5	0.1	0.023	4.1711	2.67	29.1
26.4	70.0	35	33.0	32.6	0.4	0.024	4.1711	11.13	31.8
26.7	70.0	41	37.8	37.3	0.5	0.025	4.1704	14.47	35.5
27.1	70.0	30	29.3	29.2	0.1	0.023	4.1711	2.67	29.1
27.3	70.0	35	33.0	32.8	0.4	0.024	4.1711	11.13	32.1
27.8	70.0	41	37.8	37.3	0.5	0.025	4.1704	14.47	35.8
28.1	70.0	30	29.7	29.6	0.1	0.023	4.1711	2.67	29.6
28.3	70.0	35	33.2	33.0	0.2	0.024	4.1711	5.56	32.4
28.8	70.0	41	38.0	37.5	0.5	0.025	4.1704	14.47	36.2
28.2	70.0	30	29.4	29.3	0.1	0.024	4.1711	2.78	29.7
29.2	70.0	35	33.1	33.0	0.1	0.025	4.1711	2.89	32.6
29.4	70.0	41	38.0	37.6	0.4	0.026	4.1704	12.04	36.5
30.5	70.0	35	33.2	33.1	0.1	0.023	4.1711	2.67	29.7
30.5	70.0	41	38.2	38.0	0.2	0.024	4.1595	5.54	28.9
31.1	70.0	35	33.1	33.0	0.1	0.025	4.1711	2.89	30.6
31.4	70.0	41	37.8	37.5	0.3	0.024	4.1595	8.32	35.5
32.2	71.0	35	32.8	33.2	0.4	0.025	4.1711	11.58	29.1
32.2	70.0	41	37.5	37.8	0.3	0.026	4.1595	9.01	31.8
33.1	70.0	35	33.1	33.5	0.4	0.024	4.1711	11.13	36.5
33.2	70.0	41	37.6	37.8	0.2	0.025	4.1595	5.77	32.3
34.2	71.0	41	37.9	38.3	0.4	0.026	4.1595	12.01	35.8
35.1	70.0	41	38.0	37.8	0.2	0.023	4.1595	5.31	29.3

heating medium from 0.023 m³/h to 0.026 m³/h. Similar to the thermal analysis made for the first variant of the mat, simulation tests of the amount of heat emitted as a function of the heating fluid flow rate were also carried out for the second variant. Two additional flow rates of 0.01 m³/h and 0.075 m³/h were adopted. The results of the calculations are presented in Tables 7 and 8.

The heating power of the mat for the second variant (similarly as for the first variant) depends heavily on the medium flow rate and the ambient temperature.

3.2. Analysis of the cooling function of the heating-cooling mat

An analysis was carried out of the phenomenon of cooling the child's body, during therapeutic hypothermia. An experiment was performed to determine the amount of heat absorbed by the mat from the child's body. Three temperatures in a closed incubator: 35°C, 36°C, and 37°C and constant humidity of 70% were analyzed in the study. In Table 9, for temperature differences Δt from -0.5 to -1.1°C and variable medium flow rates from 0.010 m³/h to 0.075 m³/h, the amount of heat transferred varies from -4.32 to -26.06 W.

The presented experiment confirmed the possibility of using the heating-cooling mat to cool down the environment inside the textile incubator, which, as emphasized earlier, is frequently applied in controlled therapeutic hypothermia. With reference to the analysis of the heating power results obtained for the

heating and cooling mat of the textile incubator, it can be inferred that the mat, depending on different input parameters, can emit heat in the range from 1.15 W to 86.88 W. Regarding the cooling function, the mat can receive heat in the range from -4.32 to -27.96 W. This indicates a large adjustment range for the amount of heat supplied and received, which is a positive characteristic from the point of view of programming the heat balance to ensure comfort for the baby.

4. Analysis of temperature distribution on the surface of the heating-cooling mat

The analysis of temperature distribution on the mat surface was carried out in the second part of the thermal tests. The analysis was performed using two methods. In the first one, classic contact temperature sensors were used and the second was based on thermovision technique. Figure 5 shows the first variant of the mat with marked points of temperature measurements. Some examples of surface temperature distribution matrices have been presented (Figure 7).

The description of the matrices includes the following data: ambient temperature, temperature inside the incubator, and maximum temperature difference on the mat surface (marked in red). In total, 42 temperature distribution matrices were analyzed for each of the two mat variants.

[34.1; 30°C, $\Delta t = 1.2$]

Table 7. Simulation of changes in heating power of mat with two collectors with reduced flow rate $V' = 0.01$ m³/h.

Temp. inside incubator, °C	Air humidity, %	Pump temp., °C	Inlet temp., °C	Exit temp., °C	Temp. difference, Δt , K	Water flow rate V , m ³ /h	Heat ratio k , for water MJ/m ³ K	Amount of heat emitted by mat Q_{c1} , W
25.9	70	41	37.8	37.2	0.6	0.01	4.1704	6.93
26.7	70	41	37.8	37.3	0.5	0.01	4.1704	5.77
27.3	70	35	33.0	32.8	0.4	0.01	4.1711	4.62
28.8	70	41	38.0	37.5	0.5	0.01	4.1704	5.77
29.2	70	35	33.1	33.0	0.1	0.01	4.1711	1.15
31.4	70	41	37.8	37.5	0.3	0.01	4.1595	3.40
33.2	70	41	37.6	37.8	0.2	0.01	4.1595	2.30

Table 8. Simulation of changes in heating power of mat with two collectors with increased flow rate $V' = 0.075$ m³/h.

Temp. inside incubator, °C	Air humidity, %	Pump temp., °C	Inlet temp., °C	Exit temp., °C	Temp. difference, Δt , K	Water flow rate V , m ³ /h	Heat ratio k , for water MJ/m ³ K	Amount of heat emitted by mat Q_{c1} , W
25.9	70	41	37.8	37.2	0.6	0.075	4.1704	52.12
26.7	70	41	37.8	37.3	0.5	0.075	4.1704	43.43
27.3	70	35	33.0	32.8	0.4	0.075	4.1711	34.75
28.8	70	41	38.0	37.5	0.5	0.075	4.1704	43.43
29.2	70	35	33.1	33.0	0.1	0.075	4.1711	86.88
31.4	70	41	37.8	37.5	0.3	0.075	4.1595	25.99
33.2	70	41	37.6	37.8	0.2	0.075	4.1595	17.32

Table 9. Cooling heat during therapeutic hypothermia for mat with two collectors.

Temp. inside incubator, $T_{ink}, ^\circ\text{C}$	Air humidity, %	Of heating temperature $T_{pomp}, ^\circ\text{C}$	Intel temp., $^\circ\text{C}$	Exit temp., $^\circ\text{C}$	Temp. difference, $\Delta t, \text{K}$	Water flow rate, $V, \text{m}^3/\text{h}$	Heat ratio for water $k, \text{MJ}/\text{m}^3\text{K}$	Amount of heat absorbed by the mat Q_{c1}, W	Heat transfer Q_2, W
35.0	70	26	25.4	26.1	-0.7	0.021	4.1595	-16.97	-15.77
36.0	70	27	26.5	27.1	-0.6	0.021	4.1595	-14.54	-15.57
37.0	70	28	27.4	27.9	-0.5	0.021	4.1595	-12.12	-15.82
Cooling heat during therapeutic hypothermia for mat with two collectors with increased and reduced water flow rate.									
Temp. inside incubator, $T_{ink}, ^\circ\text{C}$	Air humidity, %	Of heating temperature $T_{pomp}, ^\circ\text{C}$	Intel temp., $^\circ\text{C}$	Exit temp., $^\circ\text{C}$	Temp. difference, $\Delta t, \text{K}$	Water flow rate, $V, \text{m}^3/\text{h}$	Heat ratio for water $k, \text{MJ}/\text{m}^3\text{K}$	Amount of heat transferred, Q_{c1}, WW	
35.0	70	26	25.4	26.1	-0.7	0.010	4.1595	-8.06	
36.0	70	27	26.5	27.1	-0.6	0.010	4.1595	-6.91	
37.0	70	28	27.4	27.9	-0.5	0.010	4.1595	-5.76	
35.0	70	26	25.4	26.1	-0.7	0.075	4.1595	-6.06	
36.0	70	27	26.5	27.1	-0.6	0.075	4.1595	-5.19	
37.0	70	28	27.4	27.9	-0.5	0.075	4.1595	-4.32	
Cooling heat during therapeutic hypothermia for mat with hose interlaced every other channel,									
Temp. inside incubator, $T_{ink}, ^\circ\text{C}$	Air humidity, %	Of heating temperature $T_{pomp}, ^\circ\text{C}$	Intel temp., $^\circ\text{C}$	Exit temp., $^\circ\text{C}$	Temp. difference, $\Delta t, \text{K}$	Water flow rate, $V, \text{m}^3/\text{h}$	Heat ratio for water $k, \text{MJ}/\text{m}^3\text{K}$	Amount of heat absorbed by the mat Q_{c1}, W	Heat transfer Q_2, W
35.0	70	27.0	28.3	27.4	-0.9	0.022	4.1595	-22.87	-22.87
36.0	70	28.0	28.4	27.3	-1.1	0.022	4.1595	-27.96	-26.06
37.0	70	29.0	28.4	29.4	-1.0	0.022	4.1595	-24.51	-25.90
Cooling heat during therapeutic hypothermia for mat with PVC hose with increased and reduced water flow rates.									
Temp. inside incubator, $T_{ink}, ^\circ\text{C}$	Air humidity, %	Of heating temperature $T_{pomp}, ^\circ\text{C}$	Intel temp., $^\circ\text{C}$	Exit temp., $^\circ\text{C}$	Temp. difference, $\Delta t, \text{K}$	Water flow rate, $V, \text{m}^3/\text{h}$	Heat ratio for water $k, \text{MJ}/\text{m}^3\text{K}$	Amount of heat transferred, Q_{c1}, WW	
35.0	70	27.0	27.4	28.3	-0.9	0.01	4.1595	-10.36	
36.0	70	28.0	27.3	28.4	-1.1	0.01	4.1595	-12.67	
37.0	70	29.0	28.4	29.4	-1.0	0.01	4.1595	-11.52	
35.0	70	27.0	27.4	28.3	-0.9	0.075	4.1595	-7.97	
36.0	70	28.0	27.3	28.4	-1.1	0.075	4.1595	-9.53	
37.0	70	29.0	28.4	29.4	-1.0	0.075	4.1595	-8.66	

29	30.2	29.6	29.7
29	30.2	29.6	29.7
29	30.2	29.6	29.7
29	30.2	29.6	29.7

[35; 30°C, $\Delta t = 0.4$]

30.2	29.9	29.9	29.8
30.2	29.9	29.9	29.8
30.2	29.9	29.9	29.8
30.2	29.9	29.9	29.8

[36; 30°C, $\Delta t = 0.8$]

28.4	28.8	28	28.1
28.4	28.8	28	28.1
28.4	28.8	28	28.1
28.4	28.8	28	28.1

[37; 30°C, $\Delta t = 0.7$]

31.8	31.1	31.5	31.4
31.8	31.1	31.5	31.4
31.8	31.1	31.5	31.4
31.8	31.1	31.5	31.4

[34.2; 35°C, $\Delta t = 0.1$]

32.5	32.6	32.5	32.5
32.5	32.6	32.5	32.5
32.5	32.6	32.5	32.5
32.5	32.6	32.5	32.5

[35.2; 35°C, $\Delta t = 0.6$]

32.1	32.1	32.6	32
32.1	32.1	32.6	32
32.1	32.1	32.6	32
32.1	32.1	32.6	32

[36; 35°C, $\Delta t = 0.2$]

32.3	32.1	32.3	32.1
32.3	32.1	32.3	32.1
32.3	32.1	32.3	32.1
32.3	32.1	32.3	32.1

[37; 35°C, $\Delta t = 0.3$]

33.5	33.5	33.3	33.2
33.5	33.5	33.3	33.2
33.5	33.5	33.3	33.2
33.5	33.5	33.3	33.2

[34.4; 41°C, $\Delta t = 0.6$]

35.5	36.1	35.8	35.6
35.5	36.1	35.8	35.6
35.5	36.1	35.8	35.6
35.5	36.1	35.8	35.6

[35.2; 41°C, $\Delta t = 0.7$]

35.3	36	35.4	36
35.3	36	35.4	36
35.3	36	35.4	36
35.3	36	35.4	36

[36.1; 41°C, $\Delta t = 0.7$]

35.1	35.8	35.5	35.3
35.1	35.8	35.5	35.3
35.1	35.8	35.5	35.3
35.1	35.8	35.5	35.3

[37.1; 41°C, $\Delta t = 0.5$]

36.6	37	36.5	36.5
36.6	37	36.5	36.5
36.6	37	36.5	36.5
36.6	37	36.5	36.5

Figure 7. Temperature distribution on surface of mat with hose interlaced every other channel.

The presented measurements show that for the selected 13 variants of the matrices, a “satisfactory” even temperature distribution on the mat surface was obtained, and the temperature differences equal from 0.1°C to 0.4°C. For the remaining cases, the differences are larger (substantial) and range from 0.5°C to 1.8°C. In further research-works on the heating mat, some changes will be made in its construction, to achieve more even temperature distribution on the entire surface. Figure 6 shows one of the variants of temperature distribution on the mat with two collectors: supplying and receiving the heating medium. Figure 8 presents example matrices of temperature distribution for the analyzed input data.

[34.0; 30°C, $\Delta t = 0.5$]

29.0	29.1	29.1	29.1
28.8	28.6	28.8	28.6
29.0	29.0	28.9	28.8
28.8	28.6	28.8	29.1

[35.0; 30°C, $\Delta t = 0.6$]

29.1	29.3	29.4	29.5
29.2	29.3	28.8	29.5
28.8	29.3	29.4	28.8
29.2	29.3	29.4	29.5

[36; 30°C, $\Delta t = 0.7$]

29.1	29.3	29.4	29.5
29.0	29.0	28.8	28.8
28.8	29.0	29.1	29.1
28.8	29.7	29.0	29.3

[37.0; 30°C, $\Delta t = 0.9$]

29.8	29.9	30.0	30.4
29.8	29.5	29.6	29.6
30.1	29.8	29.9	29.8
29.5	29.6	29.5	29.5

[34.1; 35°C, $\Delta t = 0.6$]

30.6	30.6	30.5	30.6
30.9	30.3	30.6	30.3
30.6	30.7	30.7	30.5
30.8	30.6	30.6	30.5

[35; 35°C, $\Delta t = 0.5$]

31.8	31.8	31.8	31.9
32.0	31.6	31.8	31.5
31.9	32.0	32.0	31.8
32.0	31.7	31.8	31.8

[36; 35°C, $\Delta t = 0.4$]

33.0	33.0	33.0	33.1
33.1	32.7	33.0	32.7
33.1	32.9	33.1	32.9
33.0	32.8	32.9	32.9

[37.1; 35°C, $\Delta t = 0.5$]

32.4	32.3	32.4	32.5
32.5	32.0	32.3	32.1
32.5	32.4	32.5	32.3
32.3	32.1	32.3	32.5

[34.2; 41°C, $\Delta t = 0.6$]

35.1	35.5	34.6	35.0
35.9	35.6	35.6	35.1
35.5	35.8	35.9	35.1
35.9	35.8	35.7	35.9

[35.1; 41°C, $\Delta t = 0.7$]

36.4	36.5	36.3	36.2
36.8	36.3	36.6	36.3
36.5	36.8	36.8	36.5
36.8	36.6	36.6	36.1

[36.1; 41°C, $\Delta t = 0.6$]

36.5	36.6	36.3	36.3
36.9	36.5	36.8	36.3
36.6	36.9	36.8	36.6
36.9	36.7	36.7	36.3

[37.1; 41°C, $\Delta t = 0.7$]

36.0	36.0	35.9	35.8
36.5	36.1	35.8	36.3
36.0	36.2	36.1	36.0
36.4	36.1	36.1	35.8

Figure 8. Temperature distribution on surface of mat with two collectors.

The measured values show that in case of the second construction, it was possible to obtain “satisfactory” even temperature distribution on the surface of the heating mat for 13 tested variants. The obtained temperature difference Δt was from 0.1°C up to 0.3°C. For the remaining cases, the difference is substantial and ranges from 0.4°C to 1.4°C. By using a heating-cooling mat with two collectors – supplying and receiving, it was possible to slightly reduce the difference in temperature distribution on the surface of the mat from [0.1; 1.8°C] to [0.1; 1.4°C]. However, temperature differences up to 1.4°C can still be observed. The aim of further construction works will be to ensure more even temperature distribution.

In addition to the construction works on the new mat structure, it was decided to conduct further research aimed at achieving uniform temperature distribution on the mat surface by optimizing the input parameters of the heating medium, namely the flow rate and temperature of distilled water.

The second method of analyzing temperature distribution on the mat surface is instrumental methodology using thermovision technique.

Infrared thermography, also known as thermovision, is an image processing technique which involves transformation of thermal radiation, recorded by a thermal imaging camera, into a thermographic image – a thermogram, which is a graphic representation of temperature distribution on the examined surface. The test was performed using a JENOPTIK VarioCAM \hat{O} HiRes infrared camera. The thermovision test was carried out in a laboratory room where air temperature equaled 23.2°C and air humidity was \approx 50%. Two heating and cooling mats were analyzed, differing in the way the hose was interlaced in the mat channels. The temperature of the heating medium was set at 41°C, 38°C, 35°C, and 30°C (by determining the temperature on the heating pump). The measuring stand was

equipped with a thermal imaging camera placed perpendicular to the surface of the tested mats.

Figure 9 presents a thermographic image – a thermogram of the heating mat where the hose supplying the heating medium (distilled water) interlaces every other channel. The temperature of the heating medium is 30°C and its flow direction is described by a vector directed from the top to the bottom of the mat. Temperature variations have been determined along lines L1 to L5 on the thermogram. The charts below the thermogram show temperature distribution along the mat. A drop in temperature can be observed from the top to the bottom of the mat.

Clear pulsatory changes have been observed for lines L1 and L2 along the edges of the mat. The minimum temperature values for the first two temperature ranges at the edges of the mat were 27.40–28.57°C, while the maximum values were in the range of 30.17–30.37°C. The next three lines (L3, L4, and L5) represented minimum temperatures in the range of 28.88–29.20°C and maximum in the range 29.94–30.11°C. The average value of temperature for the entire mat was in the range of 29.29–29.70°C. Selected areas R6 and R7 were used to determine average temperatures at different points on the mat. The upper area R6 is warmer, as its temperatures are $t_{\max} = 30.27^\circ\text{C}$, $t_{\min} = 28.78^\circ\text{C}$, and $t_{\text{sr}} = 29.72^\circ\text{C}$, while the lower area R7 is colder, with $t_{\max} = 30.25^\circ\text{C}$, $t_{\min} = 29.02^\circ\text{C}$, and $t_{\text{sr}} = 29.52^\circ\text{C}$. For average temperatures in the analyzed areas, the difference is 0.11°C. For the determined measuring points (corresponding to the location of classic temperature measurement sensors on the surface of the mat), temperatures range from 29.12°C to 29.79°C, which gives the difference $\Delta t = 0.67^\circ\text{C}$. Figure 10 shows a thermogram of a heating mat with two collectors (supplying and receiving the heating medium). The set temperature of the medium equaled 30°C.

In case of the mat with two collectors, colored stripes are visible on the thermograms of temperature distribution, and within each of the five stripes a warmer area can be seen in the upper part and a cooler one in the lower part of the stripe. Pulsatory temperature changes are illustrated by the graph under the thermogram, which shows five periods of change. These temperature differences and the nature of their changes are determined by the construction of the mat. Figure 10 indicates temperature ranges along five lines L1, L2, L3, L4, and L5 and in areas R6 and R7.

The minimum temperature values for the first two temperature ranges on the edges of the mat equaled 27.86–28.08°C, and the maximum values 28.76–29.81°C. The next three lines represented minimum temperatures from 27.47°C to 28.66°C and maximum values 29.64–29.65°C. Average temperature was within 29.05–29.27°C. For the selected areas, temperature distribution was as follows: for R6, $t_{\max} = 29.93^\circ\text{C}$ and $t_{\min} = 28.60^\circ\text{C}$, and for R7, $t_{\max} = 29.76^\circ\text{C}$ and $t_{\min} = 28.60^\circ\text{C}$.

The average temperature in the following stripes starting from the top was: for the first 29.93°C, the second 29.31°C, the third 29.10°C, the fourth 29.15°C, and the fifth 29.23°C. Temperature differences between the maximum and minimum values were

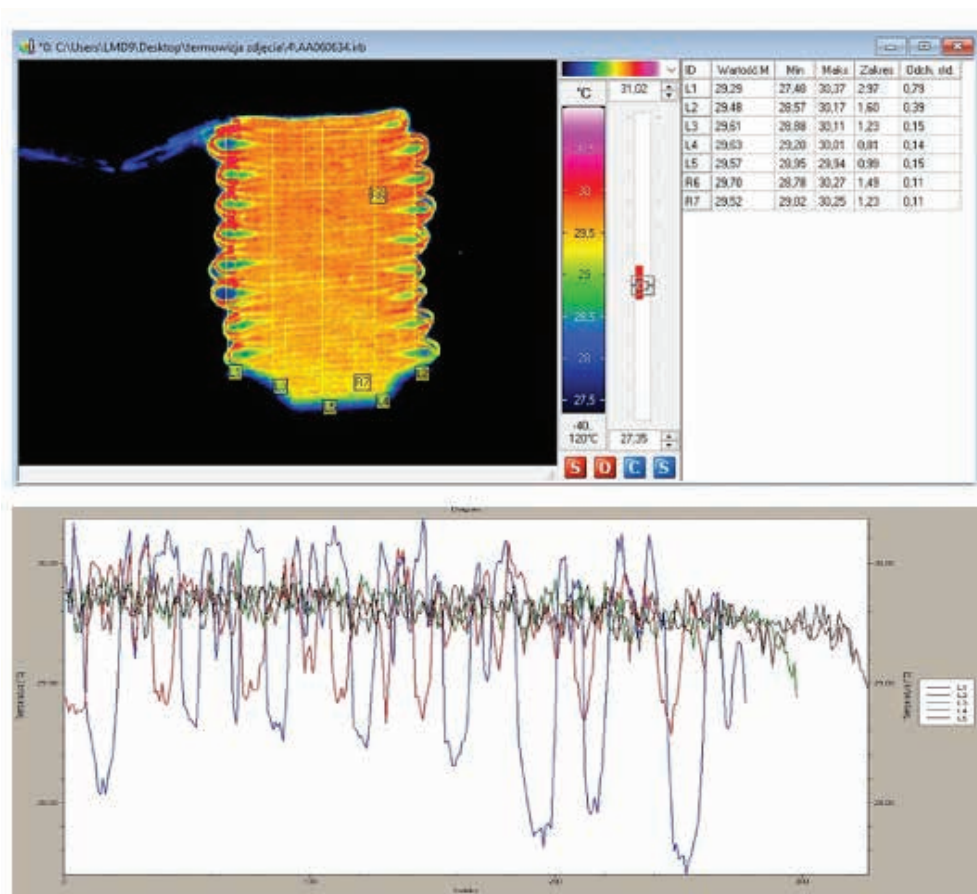


Figure 9. Temperature distribution on surface of mat with PVC hose at heating medium temperature of 30°C.

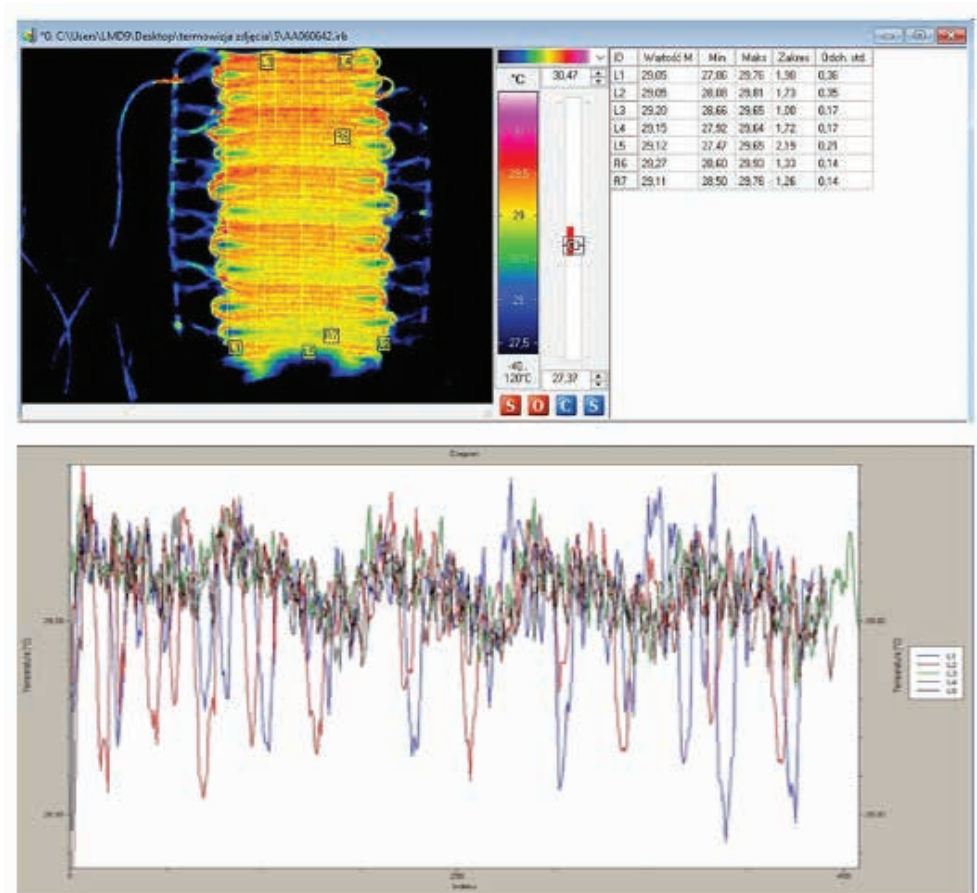


Figure 10. Temperature distribution on surface of mat with two collectors at heating medium temperature of 30°C.

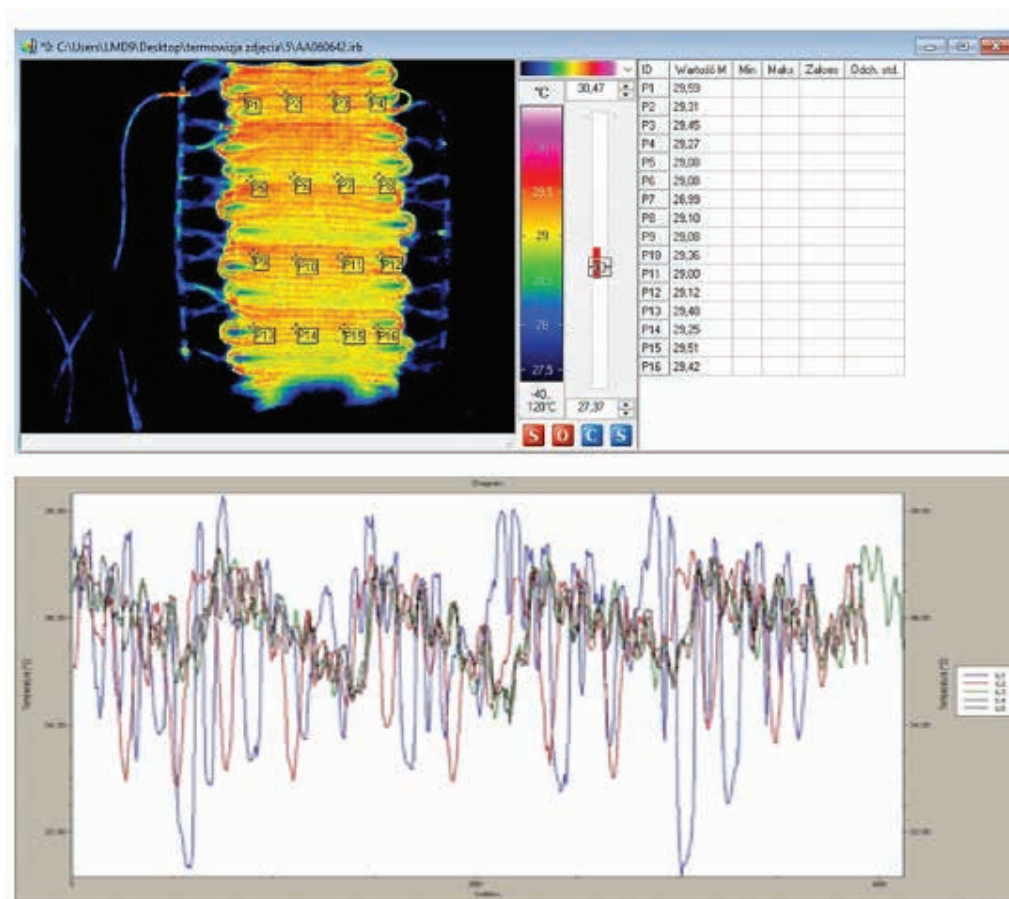


Figure 11. Temperature distribution on mat with two collectors, at heating medium temperature of 41°C.

as follows: for the first stripe 0.16°C, the second 0.11°C, the third 0.12°C, the fourth 0.15°C, and the fifth 0.14°C.

In the measuring points located on the surface of the mat with two collectors (Figure 11), when the temperature of the heating medium equaled 41°C, the temperatures ranged from 28.98°C to 29.59°C, and the temperature difference Δt was 0.61°C.

5. CONCLUSIONS

1. On the basis of the conducted literature review it was found out that a specialized active “cover” for babies and premature infants with the function of heating and cooling is available neither in Poland nor abroad. On the medical device market there are several types of stationary and portable incubators with a heating function, which can be used in the care of infants. The prototype of a textile incubator made as part of this work, which resembles “a cocoon” or “a sleeping bag” consists of five layers. The textile incubator is equipped with a functional heating and cooling mat, which is made on the basis of 3D channeled weft-knitted fabric. Its function is to generate heat and maintain it inside the textile incubator or to cool the baby’s body while using therapeutic hypothermia. Therefore, the mat is equipped with hoses transporting the heating or cooling medium.
2. Based on test results of the heating power of the heating-cooling mat intended for a textile incubator, it was found out

that the mat, depending on variable input parameters, can emit heat in the range from 1.15 W to 86.88 W. In case of the cooling function, it can receive heat in the range from -4.32 to -27.96 W. This indicates a large adjustment range of the amount of heat supplied and received, which is a positive feature, and enables programming the heat balance to ensure comfort for the baby. The effect of temperature and flow rate of the heating and cooling medium on the thermal power of the mat was also indicated.

8. The analysis of temperature measurements, made with the classic method using measuring sensors on the mat surface and using thermovision technique, confirmed that temperature distribution depends heavily on the construction of the heating mat. A characteristic feature of temperature distribution for the mat in which the hose interlaces every other channel is temperature drop along the length of the mat, from the top of the supplying hose to the bottom of the receiving one. A more favorable temperature distribution with absolute values of Δt was observed for the second variant of the mat, equipped with silicone hoses and two collectors – supplying and receiving the heating and cooling medium. For this variant, maximum temperature differences do not exceed 1.6°C. For the mat with two collectors, temperature distribution takes a striped form, depending on the number of places where the heating medium is supplied and received.

The differences in temperature distribution measured on the surface of the mat using the classic method were very

close to the values obtained with the non-contact thermal imaging method. Differences in temperature measurements according to these two methods were $\approx 0.2^{\circ}\text{C}$

References

- [1] Statistical Yearbook of the Republic of Poland. Warsaw 2019, ISSN 1506-0632.
- [2] Vakili, R., Khademi, G., Vakili, S., Saeidi, M., Emami Moghadam, Z. (2015). Child mortality at different world regions: A comparison review. *International Journal of Pediatrics*, 3(4–2), 809–816.
- [3] Schweizer, C. (2009). WHO European Centre for Environment and Health. Infant Mortality From Respiratory Diseases Fact Sheet 3.2 z December 2009 z CODE: RPG3_Air_E2. Rome, Italy 2009.
- [4] Lyon, A. (2006). Applied physiology: Temperature control in the newborn infant. *Current Paediatrics*, 16, 386–392.
- [5] Son'kin, V., Tambovtseva, R. (2012). Energy metabolism in children and adolescents. *Bioenergetics*, 121–142.
- [6] Postępy Neonatologii. *Advances in Neonatology*. No. 2, 2001. ISSN 1640 – 3959.
- [7] Lawn, J. E., Davidge, R., Paul, V. K., von Xylander, S., de Graft Johnson, J., et al. (2013). Born too soon: Care for the preterm baby. Lawn et al. *Reproductive Health*, 10(1), 1–9. doi: 10.1186/1742-4755-10-S1-S5.
- [8] Knobel, R. B., Wimmer, J. E., Jr., Holbert, D. (2005). Heat loss prevention for preterm infants in the delivery room. *Journal of Perinatology*, 25(5), 304–308.
- [9] González, M. P., Espitia, E. C. (2014). Caring for a PREMATURE child at home: From fear and doubt to trust. *Texto & Contexto-Enfermagem Nursing*, Florianópolis, 23(4), 828–835.
- [10] Roychoudhury, S., Yusuf, K. (2017). Thermoregulation: Advances in preterm infants. *NeoReviews*, 18(12), e692–e702.
- [11] McCall, E., Alderdice, F., Halliday, H., Johnston, L., Vohra, S. (2014). Challenges of minimizing heat loss at birth: A narrative overview of evidence-based thermal care interventions. *Newborn and Infant Nursing Reviews*, 14(2), 56–63.
- [12] de Almeida, M. F., Guinsburg, R., Snacho, G. A., Rosa, I. R., Lamy, Z. C., et al. (2014). Hypothermia and early neonatal mortality in preterm infants. *The Journal of Pediatrics*, 164(2), 271–275.
- [13] McCall, E. M., Alderdice, F., Halliday, H. L., Vohra, S., Johnston, L. (2018). Interventions to prevent hypothermia at birth in preterm and/or low birth weight infants. *Cochrane Database of Systematic Reviews*, 2018(2), CD004210.
- [14] Wilson, E., Maier, R. F., Norman, M., Misselwitz, B., Howell, E. A., et al. (2016). Effective perinatal intensive care in Europe (EPICE) Research Group. Admission hypothermia in very preterm infants and neonatal mortality and morbidity. *The Journal of Pediatrics*, 175, 61–67.
- [15] Baker, J. P. (2000). The incubator and the medical discovery of the premature infant. *Historical Perspective. Journal of Perinatology*, 20(5), 321–328.
- [16] Mouskou, S., Papavasileiou, P. T., Xanthos, T., Iacovidou, N. (2015). Neonatal transportation through the course of history. *Journal of Pediatrics & Neonatal Care*, 3(1), 00104.
- [17] Diamanti E Neonatal transport: International Data. *Perinatal Medicine & Neonatology*, 1(1): 41-54.2006.
- [18] Wiśniewski, S., Wiśniewski, T. S. Heat exchange. WNT, Warsaw 2013.
- [19] Ochęduszek, S. Applied thermodynamics. WNT, Warsaw 1947.
- [20] Szargut, J. Thermodynamics. PWN, Warsaw 1982.
- [21] Sobieski, W. Thermodynamics in experiments. Olsztyn 2015.